COLOR CONVERSION AND WATER SHED SEGMENTATION FOR RGB IMAGES

M. HARITHA
Dept. of ECE, JNTU College of Engineering and Technology, Anantapur, AP,India, m.harithaece@gmail.com

RAVI SHANKAR REDDY
Dept. of ECE, JNTU College of Engineering and Technology, Anantapur, AP,India,
ravishankarreddy_c@yahoo.co.in

Follow this and additional works at: https://www.interscience.in/ijess

Part of the Electrical and Electronics Commons

Recommended Citation

COLOR CONVERSION AND WATER SHED SEGMENTATION FOR RGB IMAGES

M.HARITHA[1] & RAVI SHANKAR REDDY[2]

[1,2]Dept. of ECE, JNTU College of Engineering and Technology, Anantapur, AP,India
Email: m.harithaece@gmail.com, ravishankarreddy_c@yahoo.co.in

Abstract: In this paper we describes the conversion preserves feature discriminability and reasonable color ordering, while respecting the original lightness of colors, by simple optimization of a nonlinear global mapping. Experimental results show that our method produces convincing results for a variety of color images. The required luminance adjustments are small and always lie within 1% of the mean luminance. Since all adapting lights are of the same luminance, zero luminance adjustments (dashed lines) are predicted for the asymmetric color matches under the hypothesis that adaptation is confined to the L–2M, the S – (L + M) and the L + 2M.The recovery of shape from texture under perspective projection. This is made possible by imposing a notion of homogeneity for the original texture, according it which the deformation gradient is equal to the velocity of the texture gradient equation this work studies a method called Normalized Cut and proposes an image segmentation strategy utilizing two ways to convert images into graphs: Pixel affinity and watershed transform.

I. INTRODUCTION

The color-to-gray conversion is required in many applications [1], including black-and-white printing, single channel image processing, and non-photorealistic rendering with black-and-white media. The conversion should preserve the appearance of original color images in the resulting gray-scale images. Unfortunately, a traditional method using the intensity channel (e.g., CIE Y) may fail to achieve this goal by losing feature discriminability in iso-luminant regions.

To retain feature discriminability in color-to-gray conversion, color differences in the input image should be reflected as much as possible onto the converted gray-scale values. Several color-to-gray conversion methods have been proposed, which can be divided into two main categories: local mapping and global mapping [2]. In a local mapping method, the color-to-gray mapping of pixel values is spatially varying, depending on the local distributions of colors.

Although a local mapping has advantages in accurately preserving local features, constant color regions could be converted in homogeneously if the mapping changes in the regions (Fig. 1(b)).

In a global mapping method, the same color-to-gray mapping is used for all pixels in the input. It consistently maps the same colors to the same grayscale values over an image, guaranteeing homogenous conversion of constant color regions. However, it would be more challenging to `determine such a global mapping that preserves local features at different locations at the same time (Fig. 1(c)).
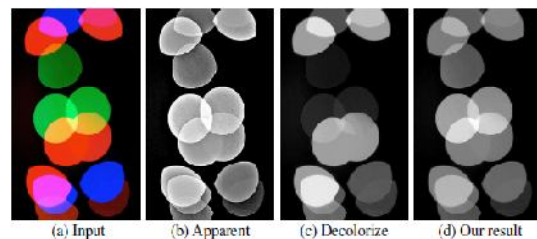

Figure 1: Comparison of color-to-gray image conversion results. (a) Input image. (b) Local mapping. (c) Linear global mapping. (d) Nonlinear global mapping.

The color-to-gray conversion algorithm considers the following criteria to preserve the visual appearance [3] of a color image:

- ☐ mapping consistency: Same colors should be mapped to the same gray-scale values.
- ☐ Feature preservation: Features in the color image should remain discriminable in the gray-scale image.
- ☐ Ordering preservation: Reasonable ordering of colors should be respected in their converted gray-scale values.
- ☐ Lightness fidelity: Color and gray-scale images should have similar lightness stimuli.

The notion of using Planckian radiators as a yardstick against which to judge other light sources is not a new one [4]. In 1923, writing about "grading of illuminants with reference to quality of color…the temperature of the source as an index of the quality of color", Priest essentially described CCT as we understand it today, going so far as to use the term apparent color temperature, and astutely recognized three cases[5]:

☐ those for which the spectral distribution of energy is identical with that given by the Planckian formula."

☐ "Those for which the spectral distribution of energy is not identical with that given by the Planckian formula, but still is of such a form that the quality of the color evoked is the same as would be evoked by the energy from a Planckian radiator at the given color temperature."

☐ "Those for which the spectral distribution of energy is such that the color can be matched only approximately by a stimulus of the Planckian form of spectral distribution."

When observing a static monocular image, we perceive the 3D structure of a scene through a combination of shape cues, especially shading, occlusion, and texture. Shape from texture, first introduced 50 year ago by Gibson[6], studies the recovery of the 3D coordinates of a surface in a scene, by analyzing the distortion of its texture projected in an image [7][8][9][10].

The shaoe from texture problem is generally broken down into two independent steps. The first step is to measure the texture distortion in the image and the second is to recover the surface coordinates from this texture distortion. Segmentation is performed by combining wavelet and watershed transform. If only watershed algorithm be used for segmentation of image, then we will have over clusters in segmentation [11]. To solve this, we used an approach. First we used the wavelet transformer to produce initial images, then watershed algorithm was applied for segmentation of the initial image, then by using the inverse wavelet transform, the segmented image was projected up to a higher resolution, in this way, we could only capture the large objects. Since wavelet decomposition involves low-pass filter, the amount of the noise can be decreased in image which in turn could lead to a robust segmentation.

II. BACKGROUND

In the past several decades, the most popular fault model used in practice is the single stuck-at fault model. In this model, one of the signal lines in a circuit is assumed to be stuck at a fixed logic value, regardless of what inputs are supplied to the circuit. Hence, if a circuit has n signal lines, there are potentially 2n stuck-at faults defined on the circuit, of which some can be viewed as being equivalent to others. The stuck-at fault model is a logical fault model because no delay information is associated with the fault definition. It is also called a permanent fault model because the faulty effect is assumed to be permanent, in contrast to intermittent faults which occur (seemingly) at random and transient faults which occur sporadically, perhaps depending on operating conditions (e.g. temperature, power supply voltage) or on the data values (high or low voltage states) on surrounding signal lines.

The single stuck-at fault model is structural because it is defined based on a structural gate-level circuit model.

A pattern set with 100% stuck-at fault coverage consists of tests to detect every possible stuck-at fault in a circuit. 100% stuck-at fault coverage does not necessarily guarantee high quality, since faults of many other kinds—such as bridging faults, opens faults, and transition (aka delay) faults—often occur.

Combinational ATPG:
The combinational ATPG method allows testing the individual nodes (or flip-flops) of the logic circuit without being concerned with the operation of the overall circuit. During test, a so-called scan-mode is enabled forcing all flip-flops (FFs) to be connected in a simplified fashion, effectively bypassing their interconnections as intended during normal operation. This allows using a relatively simple vector matrix to quickly test all the comprising FFs, as well as to trace failures to specific FFs.

Sequential ATPG:
Sequential-circuit ATPG searches for a sequence of vectors to detect a particular fault through the space of all possible vector sequences. Various search strategies and heuristics have been devised to find a shorter sequence and/or to find a sequence faster. However, according to reported results, no single strategy/heuristic out-performs others for all applications/circuits. This observation implies that a test generator should include a comprehensive set of heuristics.

Even a simple stuck-at fault requires a sequence of vectors for detection in a sequential circuit. Also, due to the presence of memory elements, the controllability and observability of the internal signals in a sequential circuit are in general much more difficult than those in a combinational logic circuit.

These factors make the complexity of sequential ATPG much higher than that of combinational ATPG, where a scan-chain (i.e. switchable, for-test-only signal chain) is added to allow simple access to the individual nodes.

III. SYSTEM DESIGN MODEL

A. Color conversion system
Before the advent of powerful, personal computers, it was common to estimate the correlated color temperature by way of interpolation from look-up tables and charts.[2]
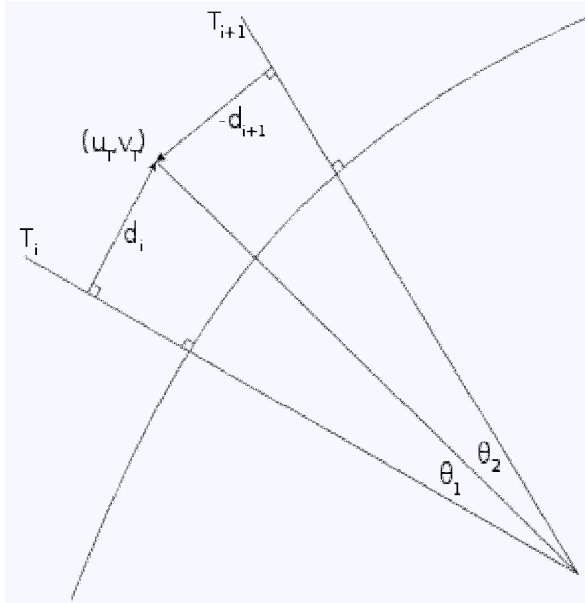
Fig: 2.Computation of the CCT T_c corresponding to the chromaticity coordinate (u_T, v_T) in the CIE 1960 UCS.

The most famous such method is Robertson's,[2] who took advantage of the relatively even spacing of the mired scale (see above) to calculate the CCT T_c using linear interpolation of the isotherm's mired values:[28]

$$\frac{1}{T_c} = \frac{1}{T_i} + \frac{\theta_1}{\theta_1 + \theta_2}\left(\frac{1}{T_{i+1}} - \frac{1}{T_i}\right)$$

where T_i and T_{i+1} are the color temperatures of the look-up isotherms and i is chosen such that $T_i < T_c < T_{i+1}$. (Furthermore, the test chromaticity lies between the only two adjacent lines for which $d_i/d_{i+1} < 0$.)

If the isotherms are tight enough, one can assume $\theta_1/\theta_2 \approx \sin\theta_1/\sin\theta_2$, leading to

$$\frac{1}{T_c} = \frac{1}{T_i} + \frac{d_i}{d_i - d_{i+1}}\left(\frac{1}{T_{i+1}} - \frac{1}{T_i}\right)$$

The distance of the test point to the i'th isotherm is given by

$$d_i = \frac{(v_T - v_i) - m_i(u_T - u_i)}{\sqrt{1 + m_i^2}}$$

where (u_i, v_i) is the chromaticity coordinate of the i'th isotherm on the Planckian locus and m_i is the isotherm's slope. Since it is perpendicular to the locus, it follows that $m_i = -1/l_i$ where l_i is the slope of the locus at (u_i, v_i).

B. Apparatus and subjects

Two subjects, the author and a naive observer, participated in the experiment. Both subjects had normal color vision. The experiments with subject

SMW were run on an Adage frame buffer controller and the stimuli were displayed on a Tektronix 690SRcolor monitor. For subject RP, the stimuli were displayed on a Barco Calibrator television monitor and computer-controlled by a modified Vista board employing the Post q operating system. Experiments were run in a dark room and only the screen of the monitor was visible. The viewing distancewas 1 m. The mean luminance was kept constant throughout the experiment at approximately35 cd/m2.

C. Calibration

The power spectrum of the phosphor primaries were measured with a Spectroradiometer (Photo Research PR- 700-SpectroScan) which outputs the CIE 1931 (2 deg field) tristimulus values based upon the Judd-modified V(l) function. The Smith and Pokomy transformation (Smith &Pokorny, 1972) was used to obtain the L, M and S cone signals for each phosphor. For the BARCO monitor, the CIE chromaticity coordinates (x,y) and the maximum luminance for the red phosphor were: X = 0.619, y = 0.348, maximum luminance= 19.65 cd/m2; for the green phosphor: x = 0.3, y = 0.592, maximum luminance= 44.90 cd/m2; for the blue phosphor: x = 0.15, y = 0.069; maximum luminance = 5.52 cd/m2.The chromaticitiesfor the Tektronix color monitor were very similar.

The conversions from CIE space to cone space were done for each monitor separately, hence taking into account the small differences in the chromaticity coordinates. Luminance was defined by the CIE 1931 standard observer, that is, iso-luminanceis defined as photometric iso-luminance using the Judd-modified V(A) function. Since the precise knowledge of the iso-luminance point was not crucial in the present experiments, the iso-luminance point was not measured for each individual observer by heterochromatic flicker photometry; the major purpose was to study chromatic adaptation without substantial adaptation effects due to luminance differences.

D. Spatial and temporal structure of stimuli

The spatial structure of the stimuli is shown in Fig. 2(a). This figure depicts the arrangement of the adapting lights (a, P) and the test (AT) and match (AM)increments on the screen. Adapting light a was always identical to the grey background; the other adapting light (B) was always chromatic. Between the two adapting lights was a smooth chromatic ramp ranging from the adapting light u (always grey) to the color of the adapting light ~. Test (T= a + AT) and match (M=/?+ AM)lights were discs with a 0.5 degree diameter.

The chromatic adapting light (~) was a two-dimensional Gaussian with an aspect ratio of 2:1; hence it looked like a vertically elongated ellipse with blurred edges slowly fading into grey.
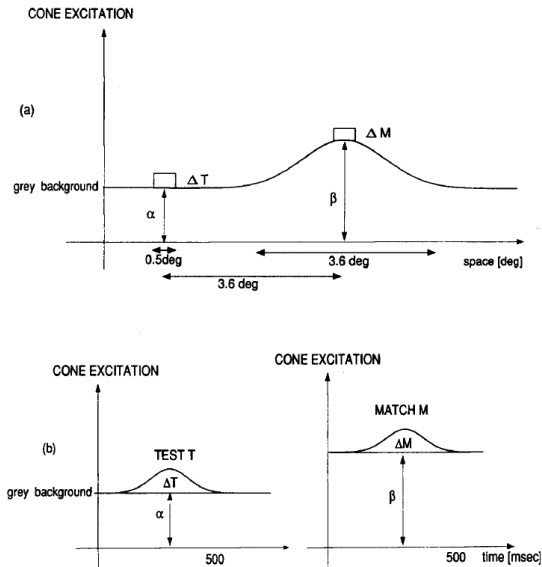
Fig: 3. Spatial and temporal properties of test, match and adapting stimuli (a) Spatial profile (b) Time course.

A dark dot of 2 min diameter was present continuously between test and match lights and served as a fixation target. Informal observations suggested that a smooth spatial onset and offset of the adapting light facilitates adaptation, that is, in most cases the entire chromatic adapting area fades to grey within less than 1min. Under these conditions, when small eye movements occurred, adaptation usually remained stable and the chromatic adapting light continued to look grey. A smooth transition between the adapting lights has a very similar effect to stabilizing the image on the retina (Krauskopf, 1963). Edges are important in determining the color appearance of an image and when no edges are provided+ ither due to retinal stabilization or a smooth onset and offset-the color within the

E. Color Segmentation

The aim of color-space transformation is to increase the separability between skin and non-skin classes while decreasing the separability among skin tones. Hopefully it will bring robust performance under varying illumination conditions. However, there are many color-spaces to choose from and a large number of metrics to judge whether they are effective.

Some potential color-spaces that we were interested in :

- CIEXYZ
- CIEXYZ
- YCbCr
- YUV
- YIQ

A performance metric that others have used includes the computation of the separability of clusters of skin and non-skin pixels using scatter matrices. Another is to do a histogram comparison of the skin and non-skin pixels after colorspace transformation. The

YCbCrcolorspace was found to perform very well in 3 out of the 4 peformance metrics used1, so we decided to use it in our color segmentation algorithm. Here is the equation for transforming from RGB to YCbCr.

$$\begin{bmatrix} Y \\ Cb \\ Cr \end{bmatrix} = \begin{bmatrix} 16 \\ 128 \\ 128 \end{bmatrix} + \begin{bmatrix} 65.481 & 128.553 & 24.966 \\ -37.797 & -74.203 & 112 \\ 112 & -93.786 & -18.214 \end{bmatrix} \begin{bmatrix} R \\ G \\ B \end{bmatrix}$$

To transform back…

$$\begin{bmatrix} R \\ G \\ B \end{bmatrix} = \begin{bmatrix} 0.00456621 & 0 & 0.00625893 \\ 0.00456621 & -0.00153632 & -0.00318811 \\ 0.00456621 & 0.00791071 & 0 \end{bmatrix} \left(\begin{bmatrix} Y \\ Cb \\ Cr \end{bmatrix} - \begin{bmatrix} 16 \\ 128 \\ 128 \end{bmatrix} \right)$$

This is a plot of the skin distribution against Cr and Cb in the YCbCrcolorspace. If the sample size is large enough, it will be a probability distribution for the image. However, our data was restricted to the training pictures we had and we did our best to find the best filter. Attempts were made to retrieve online databases for reference to generalize our filter, however it was found that the values that work best were still those derived from the training data at the loss of generalization.After extracting the pixels based on their color values, we performed the following binary operations on the color mask to remove noise:

- Close
- Fill holes
- Remove small areas
- Texture Filtering using variance thresholding

Aspect ratio criterions are found to be unreliable because the faces are too clustered, and may give false aspect ratios on regions. Binary operations, when applied in excess, will cause us to lose generality of the mask and give good results only for a specific image. Thus we discarded the former and used the latter sparingly, especially erode and dilate operations since it was impossible to justify the structuring elements used and the number of operations performed convincingly.

IV. SEGMENTATION USING WATERSHED AND NORMALIZED CUT

A. Pixel affinity

The overall quality of the segmentation depends on the pair wise pixel affinity graph. The chosen properties were the intensity and position approach presented. In this formulation, each pixel corresponds to one node in a graph. Because the graph must be not cyclic, the affinity between
a pixel and itself is 0. Equation (1) shows the formula to calculate the affinity matrix WI (i, j).

$$W_I(i, j) = e^{-\|X_i - X_j\|^2/\sigma_x - \|C_i - C_j\|^2/\sigma_C}$$

where Xi and Xj are vectors containing the x,y positions of the pixels i and j; Ci and Cj are vectors containing theRGB values (or gray-level values) of these same pixels.

B. Watershed Transform

We consider the gradient image as a topographic surface. In the watershed method, an image is segmented by constructing the catchment basins of its gradient image. The gradient image is flooded starting from selected sources(regional minima) until the whole image has been flooded.
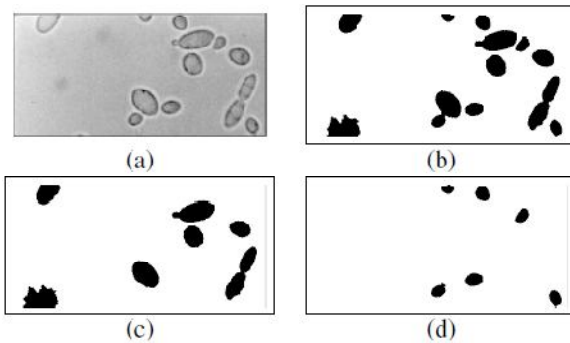

Figure 4. (a)Yeast original image; (b) yeast segmentation by WT and N-Cut; (c), (d) yeast segmentation grouped by area.

A dam is erected between lakes that meet with others lakes. At the end of the flooding process, we obtain one region for each catchment basin of the gradient image. Hierarchical Watershed creates a set of nested partitions, i.e., a hierarchy. In this case, a partition at a coarse level is obtained by merging regions of the fine partition. The watershed problem can be modeled using graphs. The gradient image is represented by a weighted neighborhood graph, where a node represents a catchment basin of the topographic surface.

We use Hierarchical Watershed in order to reduce the number of nodes (super segmentation problem)in the correspondent graph. After the conversion, we use the area and average gray-scale level of each region to set the edges weights between them.

V. RESULTS AND CONCLUSIONS

In this paper, we have presented and analyzed a method for reducing switching activity during scan shift by freezing a small subset of all flip-flops at the RTL. We have shown that large reductions in switching activity can be achieved with very low-area overhead. The amount of scan flip-flops that are going to be frozen can be decreased/increased depending on the design's overhead budget. In comparison with previous methods, which freeze these flip-flops at the gate level, timing closure can be more easily met. When flip-flops are frozen at the gate level, as was done in [40], individual timing analysis have to be implemented to determine whether or not each flipflop could be frozen without

violating timing. By freezing all flip-flops simultaneously at the RTL, we allow the synthesis tool to automatically optimize for timing closure.
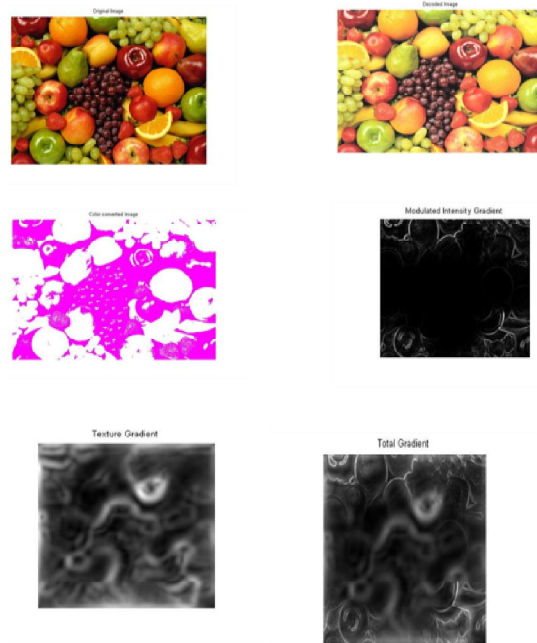

Figure 5. Simulation Results

VI. CONCLUSION

It is concluded that the method, which involves multi-resolution template matching, region clustering and color segmentation works with high accuracy with the training images which actually reflect conditions due to the high clustering factor of the faces, presence of profile faces, rotated faces etc. we have introduced an estimator for the deformation gradient and demonstrated the shape from texture algorithm on photographs. Once you can represent the problem using a graph and determine the similarity matrix, the grouping algorithm will be similar. In this way, the properties chosen to compute the edge's weights are import ants for the final result. In order to improve our results, future works can combine the image conversion methods presented and consider the region's shape as a similarity criterion.

ACKNOWLEDGEMENTS

REFERENCES

[1] BALA, R., AND ESCHBACH, R. 2004. Spatial color-to-grayscaletransform preserving chrominance edge information. In Proc.Color Imaging Conference 2004, 82–86.

[2] ADⴑ K, M. 2008. Perceptual evaluation of color-to-grayscaleimage conversions. Computer Graphics Forum (Proc. PacificGraphics 2008) 27, 7, 1745–1754.

[3] GRUNDLAND, M., AND DODGSON, N. A. 2007. Decolorize:Fast, contrast enhancing, color to grayscale conversion. Pattern Recognition 40, 11, 2891–2896.

[4] Hyde, Edward P. (June 1911). "A New Determination of the Selective Radiation from Tantalum (abstract)". Physical Review (Series I) (The American Physical Society) 32 (6): 632–633.

[5] Priest, Irwin G. (1923). "The colorimetric and photometry of daylight and incandescent illuminants by the method of rotatory dispersion". JOSA 7 (12): 1175–1209.

[6] J.Gibson, the perception of the visual world.boston, mass.: Houghton mifflion,1950.

[7] J.Garding," shape from texture for smooth curved surfaces in perspective projection,"J.math imaging vision, vol, pp.327-350,1992.

[8] W Hwang, C.-S.Lu, and P.-C. Chung, "Shape from texture: Estimation of Planar Syrface Orientation through the Ridge Surfaces of Continuous Wavelet Transform," IEEE trans. Image Processing, vol.7, pp. 773-780, 1998.

[9] K. Kanatani and T. Chou,"shape from texture : General principle," artificial intelligence, vol.38,pp.1-48,1989.

[10] J.Malik and R.Rosenholtz,"Computing local surface orientation and shape from texture for curved surfaces," int'l J.computer vision, vol.23, no.2, pp.149-168, 1997.

[11] Beaulieu, J. M., Touzi, R., "Segmentation of Textured Polarimetric SAR Scenes by Likelihood Approximation", IEEE TRANSACTIONS ON GEOSCIENCE AND REMOTE SENSING, VOL. 42, NO. 10, OCTOBER 2004

❖ ❖ ❖